OPTIMAL OFFSET AVERAGING FOR FLASH AND FOLDING A/D CONVERTERS

Ovidiu Carnu and Adrian Leuciuc

Stony Brook University
Department of Electrical and Computer Engineering
Stony Brook, NY 11794

ABSTRACT

Resistive networks can be used as spatial filters to average the random errors in arrays of analog cells, specifically for decreasing the offsets in flash and folding A/D converters. In this communication the critical conditions the averaging networks have to satisfy are pointed out and the optimal topology, order, and parameters of the resistive grids are identified for each of the two ADC architectures.

1. INTRODUCTION

Flash and folding architectures represent two of the implementation approaches for high-speed A/D converters (ADC). Flash ADCs do not require front-end sample-and-hold amplifiers and this makes them the best approach for high-speed applications. However, the flash architecture is limited to low resolutions because of the exponential dependence of the dissipated power and die area on the effective number of bits. The folding ADCs use analog signal preprocessing to decrease the number of comparators in a flash-type converter. The folding operation reduces however the maximum frequency of the signals that can be converted, drawback that can be eliminated by a front-end track-and-hold circuit (with its own limitations and disadvantages).

In both flash and folding architectures there is always a trade-off between speed and accuracy. Thus, by decreasing the sizes of the transistors used in the input stages one can increase the conversion rate, but at the expense of larger input offsets, therefore reduced accuracy. An effective technique for decreasing the offsets in an array of amplifiers was initially proposed in [1] in the case of a flash ADC. Lateral resistors have been inserted between the preamplifier outputs of adjacent comparators to average their random offsets while maintaining their speed. This technique has been used in other subsequently reported implementations of both flash and folding ADCs [2]-[6]. A complete and thorough analysis of the averaging mechanism in the case of flash ADCs has been presented in [7], the authors proposing also an algorithm to optimally design a flash and averaging ADC. All the references cited above are using only first-order resistive networks for averaging. In [8] it has been shown that improved performance can be achieved with a second-order active resistive spatial filter for offset averaging. All the results presented in this communication refer to the case of second-order resistive networks.

This work was supported by the Center for Design of Analog/Digital Integrated Circuits CDADIC

2. FRONT-END STAGES OF FLASH AND FOLDING A/D CONVERTERS

To better understand the offset averaging technique we need to correctly identify the problem. Figures 1 and 2 respectively, show the input stages of the flash and folding ADC architectures, including the offset averaging networks. The preamplifiers (flash ADC) or folding amplifiers (folding ADC) inject currents into the averaging resistive network and the voltage at a specific output node is set by the contribution of all cells in the array.

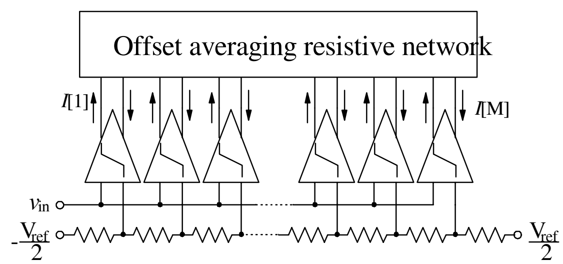

Fig. 1. Input stage of a flash ADC.

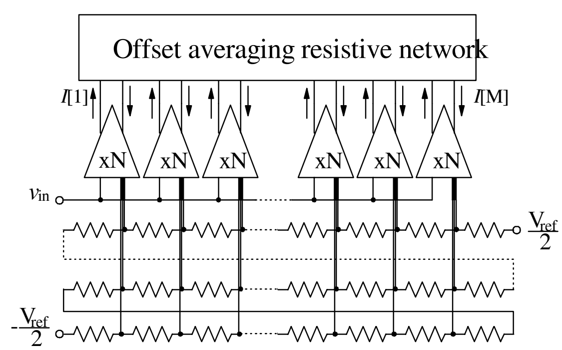

Fig. 2. Input stage of a folding ADC.

The global spatial distribution of the output currents for both architectures is shown on top of Fig. 3. In the same figure the spatial distribution of currents for a specific value of the input voltage is depicted, the input voltage having values in the mid, lower, and respectively upper range. For the same number of zero crossings the folding architecture has less cells in the input stage than the flash ADC, decreased by the folding rate. Whereas this consists the main advantage of the folding architecture in terms of power dissipation and die area, it may be a drawback from the point of view of offset averaging. When mismatches are

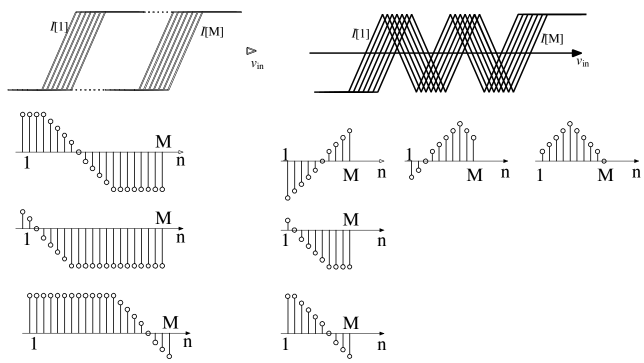

(a) Flash ADC (b) Folding ADC

Fig. 3. Current distribution for the flash and folding ADCs.

considered, the ideal current samples shown in Fig. 3 will be affected by random errors, which can be seen as spatially distributed white noise. The offset averaging network acts as a spatial filter that should (i) remove as much as possible the errors and (ii) preserve the ideal zero-crossings of the input signal. As it will be shown in the next sections, depending on the topology of the averaging network, these two conditions can be opposed to each other. At the same time, the offset averaging network should not affect (to a great extent) the gain of the individual amplifiers.

3. OFFSET AVERAGING NETWORKS AS SPATIAL FILTERS

A section of a second-order offset averaging resistive network is shown in Fig. 4, in a single-ended version. The amplifiers are represented by current sources in parallel with resistors R_0 modeling their finite output resistance. A nodal analysis leads to the following difference equation

$$\begin{aligned} y[n] &= a(y[n-1]+y[n+1]) + b(y[n-2]+y[n+2]) + \\ &+(1-2a-2b)x[n], \qquad (1) \end{aligned}$$

where

$$a = \frac{G_1}{G_0+2G_1+2G_2},\ b = \frac{G_2}{G_0+2G_1+2G_2}$$

and $x[n] = R_0 I[n]$ is the voltage at node n in the absence of lateral resistors. In the case of an infinite network, the node voltages $y[n]$ are given by the convolution product between the input $x[n]$ and the symmetrical two-sided impulse response $h_{\inf}[n]$ obtained by inverse Z-transform from the transfer function

$$H(z) = \frac{(1-2a-2b)}{1-a\left(z+z^{-1}\right)-b\left(z^2+z^{-2}\right)} \qquad (2)$$

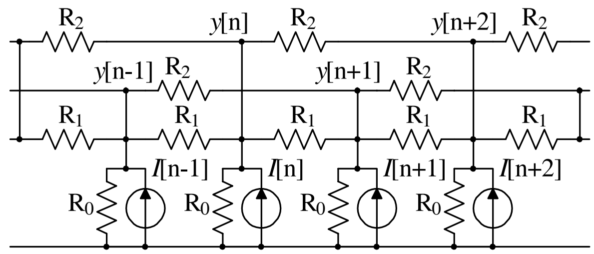

Fig. 4. Second-order resistive spatial filter.

The spatial stability of the infinite resistive network described by (1) and the properties of its frequency response have been analyzed in [9]. It has been shown that a maximally flat low-pass filter can be obtained if $a = -4b$ and $0 < a < 2/3$. The -3dB spatial bandwidth of the maximally flat filter is given by

$$\cos(\omega_{-3dB}) = 1 + \frac{\sqrt{\left(2-\sqrt{2}\right)a\left(2-3a\right)}}{2a}$$

An infinite network will ensure the zero crossings of the output voltages $y[n]$ correspond to the ones of the input currents $I[n]$ (odd symmetrical input convoluted with an even symmetrical impulse response). However, in the case of finite resistive grids different boundary conditions will generate more or less, smaller or larger errors in the zero crossings of the outputs.

4. EFFECT OF BOUNDARY CONDITIONS

There are various approaches of obtaining a finite resistive grid from an infinite one, corresponding to different boundary conditions imposed on the difference equation (1). One can terminate the network in open-circuit, in short-circuit, or using a resistive termination. Another possibility is the ring connection in which one end of the network is connected to the other end. This last configuration and the resistive termination using an optimal resistive two-port [10] are the only ones with a shift-invariant convolution kernel $h[n]$. However, none of the obtained finite networks will preserve the correctness of the zero-crossings with the exception of the center one. This is justified by the fact that, even in the case of an even symmetrical impulse response, the input samples are disposed symmetrically only around the center zero crossing (see Fig. 3). Therefore, depending on how quickly the impulse response decays, the errors in the zero crossings introduced by the edge effect will be smaller or larger. This effect is amplified in the case of the folding architecture where the number of cells is reduced. Simulation results showing the errors of the output zero crossings for various boundary conditions are plotted in Fig. 5. For both the flash and folding architectures a number of 80 zero crossings has been chosen and 16 cells are operating simultaneously in the linear region. The parameters (a, b) of the network have been computed to correspond to a maximally flat second-order spatial filter with bandwidth of $\pi/32$. Obviously, one can always choose the parameters of the spatial filter in such a way that the errors are below an imposed INL value. However, this usually means either a poor offset averaging or a significant decrease in the gain of amplifiers. Nevertheless, there is one possible network

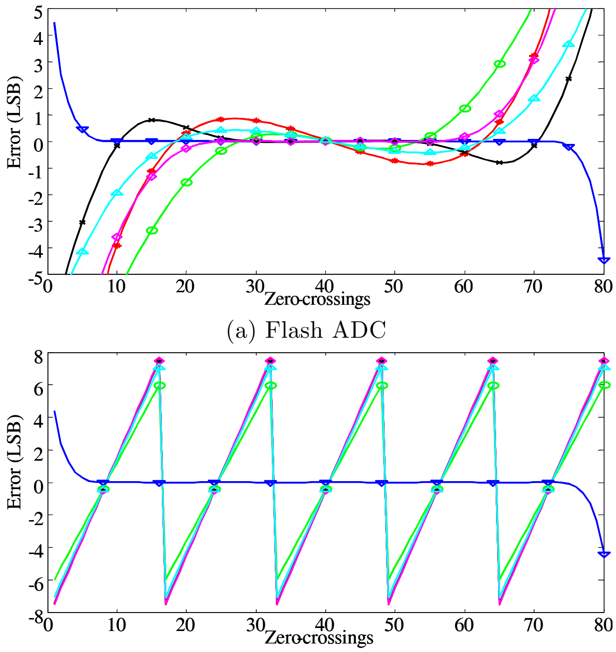

(a) Flash ADC

(b) Folding ADC

Fig. 5. Effect of boundary conditions: ○ - short-circuit; × - open-circuit; △ - optimal resistive termination; ⋄ - constant; ∗ - ring; ∇ - Moebius.

configuration which eliminates most of the zero-crossing errors. One can always take advantage of the fully differential implementation of the input stage to build a Moebius-like topology in which the ends of the resistive strings connecting the non-inverting outputs of the amplifiers is connected to the opposite ends of the resistive strings connecting the inverting inputs, and the other way round. This way, one obtains a 2M-length ring-connected network with an odd symmetrical distribution of input samples (excepting the ends where some amplifiers are not yet in linear region). The output zero crossings will correspond to the input zero crossings, except for a finite number which does not depend on filter parameters, but only on the number of cells which are simultaneously operating in the linear region. This case is also depicted in Fig. 5.

5. OPTIMAL OFFSET AVERAGING

In the case of a M-length ring connection the convolution between the input signal and the finite convolution kernel $h[n]$ is equivalent to the M-length circular convolution between the input signal and the impulse response of the infinite network $h_{inf}[n]$. The Moebius-like resistive grid will preserve this property with the only difference that the length of the network connecting M fully differential cells is 2M. In spatial frequency domain, this operation translates to a multiplication of the 2M-point Discrete Fourier Transforms (DFT) of $h_{inf}[n]$ and of the input signal : $Y[k] = H[k]X[k]$, $k = 1..2M$. The DFT of the spatial filter impulse response is obtained by sampling the frequency response (2) at $k\pi/M$, with $k = 0..2M-1$.

Moreover, for the Moebius connection the input signal is odd symmetric because it results from concatenating the spatial signal distribution (Fig. 3) with its negated version ($x[n] = -x[n+M]$, $n = 1...M$). The DFT computed for odd symmetric signals with a length of 2M yields:

$$\begin{aligned} X[k] &= 2\sum_{n=1}^{M} x[n]e^{-j\frac{\pi}{M}kn}, \quad \text{odd} \quad \text{k} \\ X[k] &= 0, \qquad\qquad\qquad\qquad \text{even} \quad \text{k} \end{aligned}$$

In a real case, offsets are added to the useful signal, and they are also odd symmetrically distributed over the network. Assuming random and uncorrelated offsets, their spatial power spectrum density will have equal odd samples and null even samples and it will sum with the ideal signal power spectrum. In the following the particular case of folding ADCs will be discussed, but the results can be applied with minor changes to flash ADCs.

For a correct functioning of the folding ADCs the input stage linearity is not important, but only the zero-crossings' accuracy. Hence, it is acceptable to change the signal shape as long as the zero-crossings are preserved. The zero-crossings are generated by the first spectral line $X[1]$ of the ideal input signal. The rest of the spectral lines do not provide any useful information and can be eliminated. This conclusion is particularly important for offset averaging and shows that a spatial filter can be used to reduce the effect of offsets. However, the offset spectral line overlapped over the useful signal cannot be removed, becoming the fundamental limitation of the spatial filtering.

One should take in account that, in a physical implementation, the value of the signal at the output of the folding amplifier cannot be too high due to the finite supply voltage. Saturation compromises the effect of spatial filtering because the saturated signal does not convey any information about the amplifier offset. Thus, the filter gain is inferred from the maximum amplitude attainable by the output signal without saturating the amplifiers. If the filter is almost ideal (i.e. the value of the first spectral line is much larger than the others), the shape of folding signal will change from triangular to sinusoidal and the filter gain is given by the amplitude of the first spectral component. The offsets of the spatial filtered signal (referred to the input) can be derived as a function of the offsets of the signal before filtering:

$$\sigma_{iy}^2 = \frac{g_x^2}{g_y^2}\frac{\sigma_{ix}^2}{M}\sum_{j=0}^{M-1}|H(2j+1)|^2 \tag{3}$$

where g_x, g_y, σ_{ix}, σ_{iy} represent the gain around a zero-crossing and, respectively, the standard deviations of the input referred offsets of the folding stage before and after filtering. To find the optimum filter, a cost function is defined as the power of offsets:

$$C(a,b) = \sum_{j=0}^{M-1}\left|H\left[(2j+1)\frac{\pi}{M}\right]\right|^2 \tag{4}$$

The problem reduces now to minimizing the cost function C with a constraint. The constraint is given by the filter gain for the useful signal, set by the value of its first spectral line:

$$H\left(\frac{\pi}{M}\right) = G \tag{5}$$

Equation (5) generates a family of lines in the (a, b) plane, all of them passing through the point (a_0, b_0) corresponding to:

$$\begin{aligned} 1 - 2a_0 - 2b_0 &= 0 \\ 1 - 2a_0\cos(\pi/M) - 2b_0\cos(2\pi/M) &= 0 \end{aligned}$$

The minimum cost is reached in the point (a_0, b_0), but the filter with coefficients a_0 and b_0 is unstable. Around (a_0, b_0) the cost function increases with distance (Fig. 6). One can choose a stable point (a, b) on the line defined by (5) as close as possible to (a_0, b_0), trading off a small penalty in offset rejection for stability and a smaller sensitivity to coefficient variations. Considering the filter almost ideal the INL improvement can be derived from (3) as:

$$INL_{imp} = \frac{\sigma_{ix}}{\sigma_{iy}} = \sqrt{\frac{M}{2}\frac{p\pi}{2}}$$

where $p = \dfrac{2}{M^2\sin^2(\pi/2M)}$ is the amplitude of the first spectral component of the normalized triangular folding signal. The DNL is measured as the difference between two adjacent quantization levels: $DNL[i] = y[i+1] - y[i]$. In frequency domain, this yields:

$$DNL(e^{j\omega}) = 2\sin\frac{\omega}{2}e^{j(\frac{\pi}{2}+\frac{\omega}{2})Y(e^{j\omega})}$$

DNL computation corresponds to a supplementary high-pass filtering of the signal. The ideal filter cancels all the high-order spectral components and also minimizes the DNL. Using the same approach as for INL improvement computation, the DNL improvement can be approximated as follows:

$$\begin{aligned} DNL_{ix} &= \sqrt{2}\sigma_{ix} \\ DNL_{oy} &= 2G\sqrt{\frac{2}{M}}\sin\left(\frac{\pi}{2M}\right)\sigma_{ox} \\ DNL_{imp} &= \frac{DNL_{ix}}{DNL_{iy}} = \frac{g_y}{g_x}\frac{DNL_{ox}}{DNL_{oy}} = \frac{\pi}{4}p\frac{\sqrt{M}}{\sin(\pi/2M)} \end{aligned}$$

The values obtained for DNL improvement are much higher because the filter introduces a strong correlation between offsets of the adjacent amplifiers.

6. CONCLUSIONS

The second order resistive grid with a Moebius-like topology is shown to be optimal in terms of minimizing the zero-crossings errors in flash and folding ADCs. Moebius topology preserves the correctness of most of the zero-crossings without limiting the offset averaging. A second order averaging grid can remove the offsets in an optimal manner for a large range of gains.

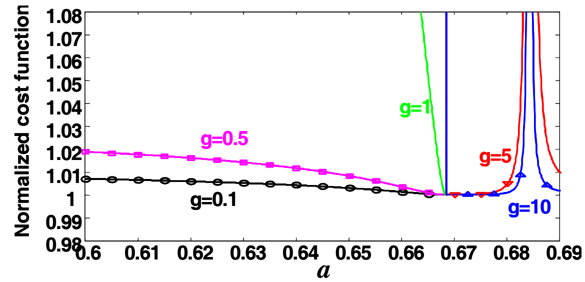

Fig. 6. Normalized cost function around the ideal point (a_0, b_0) for M=18

7. REFERENCES

[1] K. Kattman and J. Barrow, "A Technique for Reducing Differential Non-Linearity Errors in Flash A/D Converters," ISSCC Dig. Tech. Papers, Feb. 1991, pp. 170-171.

[2] P. Vorekamp and R. Roovers, "A 12-b, 60-MSamples/s Cascaded and Interpolating ADC," IEEE J. of Solid-State Circuits, vol. 32, no. 12, Dec. 1997, pp. 1876-1886.

[3] K. Bult and A. Buchwald, "An Embedded 240-mW 10-b 50-MS/s CMOS ADC in 1-mm^2," IEEE J. of Solid-State Circuits, vol. 32, no. 12, Dec. 1997, pp. 1887-1895.

[4] H. Pan, M. Segami, M. Choi, J. Cao, and A.A. Abidi, "A 3.3-V 12-b 50-MS/s A/D Converter in 0.6-μm CMOS with over 80-dB SFDR," IEEE J. of Solid-State Circuits, vol. 35, no. 12, Dec. 2000, pp. 1769-1780.

[5] M Choi and A.A. Abidi, "A 6-b 1.3-GSample/s A/D Converter in 0.35-μm CMOS," IEEE J. of Solid-State Circuits, vol. 36, no. 12, Dec. 2001, pp. 1847-1858.

[6] P.C.S. Scholtens and M. Vertregt, "A 6-b 1.6-Gsample/s Flash ADC in 0.18-μm CMOS using Averaging Termination," IEEE J. of Solid-State Circuits, vol. 37, no. 12, Dec. 2002, pp. 1599-1609.

[7] H. Pan and A.A. Abidi, "Spatial Filtering in Flash A/D Converters," IEEE Trans. Circuits and Systems-II, vol. CSII-50, no. 8, Aug. 2003, pp. 424-436.

[8] A. Leuciuc and O. Carnu - "Active Spatial Filtering for A/D Converters," Proc. of ISCAS'2002, Phoenix, 26-29 May 2002, vol. II, pp. 392-395.

[9] A. Leuciuc and O. Carnu - "On Some Properties of One-Dimensional Resistive Spatial Filters", Proc. of ECCTD'03, Krakow, Poland, 1-4 Sep. 2003, vol. II, pp. 309-312.

[10] J. White and A. N. Wilson, "On the Equivalence of Spatial and Temporal Stability for Translation Invariant Resistive Networks," IEEE Trans. on Circuits and Syst. - Part I, vol. CSI-39, no. 9, Sep. 1992, pp. 734-743.